

4-14-2022

Impaired microcirculatory function, mitochondrial respiration, and oxygen utilization in skeletal muscle of claudicating patients with peripheral artery disease

Song-young Park

Elizabeth J. Pekas

Cody Anderson

Tyler N. Kambis

Paras K. Mishra

See next page for additional authors

Follow this and additional works at: <https://digitalcommons.unomaha.edu/hperfacpub>



Part of the [Health and Physical Education Commons](#), and the [Kinesiology Commons](#)

Please take our feedback survey at: https://unomaha.az1.qualtrics.com/jfe/form/SV_8cchtFmpDyGfBLE

Authors

Song-young Park, Elizabeth J. Pekas, Cody Anderson, Tyler N. Kambis, Paras K. Mishra, Molly Schieber, TeSean Wooden, Jonathan R. Thompson, Kyung-Soo Kim, and Iraklis Pipinos

Impaired microcirculatory function, mitochondrial respiration, and oxygen utilization in skeletal muscle of claudicating patients with peripheral artery disease

Song-Young Park,^{1*} Elizabeth J. Pekas,^{1*} Cody P. Anderson,¹ Tyler N. Kambis,² Paras K. Mishra,² Molly N. Schieber,³ TeSean K. Wooden,¹ Jonathan R. Thompson,³ Kyung Soo Kim,^{3,4} and Iraklis I. Pipinos^{3,4}

¹*School of Health and Kinesiology, University of Nebraska at Omaha, Omaha, Nebraska;*

²*Department of Cellular and Integrative Physiology, University of Nebraska Medical Center, Omaha, Nebraska;*

³*Department of Surgery, University of Nebraska Medical Center, Omaha, Nebraska; and*

⁴*Department of Surgery and Veterans Affairs Research Service, Nebraska- Western Iowa Health Care System, Omaha, Nebraska*

*S.-Y. Park and E. J. Pekas contributed equally to this work.

Abstract

Peripheral artery disease (PAD) is an atherosclerotic disease that impairs blood flow and muscle function in the lower limbs. A skeletal muscle myopathy characterized by mitochondrial dysfunction and oxidative damage is present in PAD; however, the underlying mechanisms are not well established. We investigated the impact of chronic ischemia on skeletal muscle microcirculatory function and its association with leg skeletal muscle mitochondrial function and oxygen delivery and utilization capacity in PAD. Gastrocnemius samples and arterioles were harvested from patients with PAD ($n = 10$) and age-matched controls (Con, $n = 11$). Endothelium-dependent and independent vasodilation was assessed in response to flow ($30 \mu\text{L} \cdot \text{min}^{-1}$), acetylcholine, and sodium nitroprusside (SNP). Skeletal muscle mitochondrial respiration was quantified by high-resolution respirometry, microvascular oxygen delivery, and utilization capacity (tissue oxygenation index, TOI) were assessed by near-infrared spectroscopy. Vasodilation was attenuated in PAD ($P < 0.05$) in response to acetylcholine (Con: $71.1 \pm 11.1\%$, PAD: $45.7 \pm 18.1\%$) and flow (Con: $46.6 \pm 20.1\%$, PAD: $29.3 \pm 10.5\%$) but not SNP ($P = 0.30$). Complex I + II state 3 respiration ($P <$

0.01) and TOI recovery rate were impaired in PAD ($P < 0.05$). Both flow and acetylcholine-mediated vasodilation were positively associated with complex I + II state 3 respiration ($r = 0.5$ and $r = 0.5$, respectively, $P < 0.05$). Flow-mediated vasodilation and complex I + II state 3 respiration were positively associated with TOI recovery rate ($r = 0.8$ and $r = 0.7$, respectively, $P < 0.05$). These findings suggest that chronic ischemia attenuates skeletal muscle arteriole endothelial function, which may be a key mediator for mitochondrial and microcirculatory dysfunction in the PAD leg skeletal muscle. Targeting microvascular dysfunction may be an effective strategy to prevent and/or reverse disease progression in PAD.

NEW & NOTEWORTHY Ex vivo skeletal muscle arteriole endothelial function is impaired in claudicating patients with PAD, and this is associated with attenuated skeletal muscle mitochondrial respiration. In vivo skeletal muscle oxygen delivery and utilization capacity is compromised in PAD, and this may be due to microcirculatory and mitochondrial dysfunction. These results suggest that targeting skeletal muscle arteriole function may lead to improvements in skeletal muscle mitochondrial respiration and oxygen delivery and utilization capacity in claudicating patients with PAD.

chronic ischemia; endothelial dysfunction; microvascular dysfunction; peripheral artery disease

INTRODUCTION

Peripheral artery disease (PAD) is an atherosclerotic disease that impairs the blood flow and muscle function of the lower extremities (1). The prevalence of PAD increases with age and affects over 200 million individuals globally (1, 2). Symptoms of PAD typically include intermittent claudication and leg fatigue in the earlier disease stages, but as the disease progresses patients may experience critical limb ischemia (CLI; 1). Treatment options for PAD are fairly limited, with amputation being necessary for a large number of patients with CLI. Therefore, it is essential to investigate the mechanisms underlying skeletal muscle mitochondrial dysfunction, oxidative stress damage, walking capacity,

and attenuated oxygen delivery capacity in PAD to develop successful and lasting therapeutic interventions that may avert or reverse disease progression.

PAD is thought to be initiated by atherosclerotic blockages in the conduit arteries reducing blood flow to the legs. However, hemodynamic measures alone (reflective of conduit artery disease) have failed to explain the degree of functional impairment in the legs of patients with PAD. We believe that a compromised microcirculatory network is a more likely determinant of leg function, as the microcirculation is known as a key regulator of skeletal muscle blood flow and perfusion (3–6). Previous studies have shown that a myopathy characterized by skeletal muscle mitochondrial dysfunction and oxidative damage affects the muscles of the ischemic legs of patients with PAD (7, 8), but the exact mechanisms underlying these biochemical changes have not been well documented. One potential mechanism may be a failure of the downstream skeletal muscle microcirculatory network to regulate muscle blood flow and perfusion. Previous work in animal skeletal muscle microcirculation has shown that ischemia can induce the production of reactive oxygen species (ROS) in the arterioles (9), whereas ischemia-reperfusion is associated with arteriolar vasoconstriction and attenuated capillary perfusion (10), and these microvascular deficits may be key contributors to the deleterious environment that induces oxidative damage and mitochondrial dysfunction in PAD (7, 8). In support of this theory, our group and others have recently shown that patients with claudication experience abnormally fast reductions in calf muscle oxygen saturation during walking, suggesting that patients with PAD may have impaired microcirculatory function (11–13).

There are currently no studies that have used isolated skeletal muscle arterioles to directly examine the skeletal muscle microcirculation in the claudicating legs of patients with PAD, and this is likely due to limited access to tissue samples from this population. To the extent of our knowledge, this is the first study that aimed to directly examine the vasomotor function of skeletal muscle arterioles and its potential association with mitochondrial dysfunction and impaired microvascular oxygen delivery and utilization capacity in the

claudicating limbs of patients with PAD. We tested the hypotheses that in the skeletal muscles of the affected lower extremities of claudicating patients with PAD: 1) endothelium-dependent vasodilatory function is impaired, whereas endothelium-independent vasodilatory function is not altered, 2) impaired endothelium-dependent vasodilation correlates with attenuated skeletal muscle mitochondrial respiratory function, and 3) attenuated endothelium-dependent vasodilation and skeletal muscle mitochondrial respiratory function correlates with impaired oxygen delivery and utilization capacity.

METHODS

Participants

The experimental protocol was approved by the Veterans Affairs Nebraska-Western Iowa Institutional Review Boards. All subjects gave written, informed consent, and all protocols were performed in accordance with the Declaration of Helsinki. A total of 11 male control (Con) participants (Con, age 64 ± 8 yr) and 10 male patients with claudication (PAD, age 68 ± 9 yr) were recruited for participation. Con participants led sedentary lifestyles, had no history of PAD-related symptoms, and had normal blood flow to their lower limbs as indicated by normal ankle-brachial index (ABI) at rest and after stress. Patients with PAD presented with claudication (Fontaine Stage II PAD) and were undergoing evaluation for symptomatic PAD. Medical history, physical examination, decreased ABI (ABI < 0.9), and computerized or standard arteriography that revealed stenotic and/or occluded arteries supplying the lower extremity were evaluated to establish the diagnosis for each patient. All patients with PAD presented with intermittent claudication, but no ischemic rest pain or tissue loss. Participants were instructed to arrive for testing after an overnight fast.

Skeletal Muscle and Arteriole Harvest and Preparation

Gastrocnemius samples were obtained from the anteromedial aspect of the medial muscle belly 10 cm distal to the tibial tuberosity. This biopsy site was chosen because the posterior calf muscles (plantar flexors) are the muscle group

most affected by PAD-related symptoms and are consistently found to be impaired in biomechanical evaluations comparing muscle performance between patients with PAD and controls (14–16). In addition, the gastrocnemius is the most superficially located muscle of the posterior compartment of the calf, and its anteromedial aspect is easily accessed via a medial approach (14–16). All biopsies were obtained with a 6-mm Bergstrom needle (7). Samples were transported to the laboratory immediately in biopsy preservation solution [BIOPS; containing (in mM) 2.77 CaK₂EGTA, 7.23 K₂EGTA, 6.56 MgCl₂, 0.5 DTT, 50 K-MES, 20 imidazole, 20 taurine, 5.77 Na₂ATP, and 15 phosphocreatine, pH 7.1 at 4°C]. Arterioles were isolated, and skeletal muscle was prepared for permeabilization and respiratory analysis within 15 min of tissue arrival. The remaining skeletal muscle not used for the respiratory assessment was frozen at –80°C for later citrate synthase activity and immuno- blotting analyses.

Arteriole Isolation and Vasodilation Assessments

Arterioles (~30–80 µm of intraluminal diameter, 1 arteriole/participant) were isolated from the skeletal muscle using a dissection microscope (Zeiss Stemi 305 Dissection Microscope, Zeiss, White Plains, NY) in BIOPS. Any additional connective tissues and adipose tissues surrounding the arterioles were removed in 4°C physiological saline solution [PSS; containing (in mM) 145.0 NaCl, 4.7 KCl, 2.0 CaCl₂, 1.17 MgSO₄, 5.0 glucose, 2.0 pyruvate, 0.02 EDTA, and 3.0 MOPS with 10 g/L BSA at pH 7.4; 17]. Arterioles were cannulated onto glass micropipettes and mounted in myograph chambers at 37°C in PSS (Culture Myograph System, 204CM, DMT Systems, Aarhus, Denmark; 18). Arterioles were incubated and allowed to equilibrate for 1 h in the PSS solution. Vessel diameter was assessed using an inverted microscope and camera system (DMT Systems), and data were projected in real time to the automated edge-detection software (MyoVIEW, v.4, DMT Systems). Fluid leak was assessed by pressurizing the arteriole to an intraluminal pressure of 60 mmHg (17, 19). Arterioles free of leaks were used for the vasodilatory function experiments.

Briefly, vasodilatory dose-response curves (%) were assessed in response to

three different stimuli to comprehensively assess vasodilatory function: endothelium-mediated vasodilation in response to increased shear stress, endothelium-mediated vasodilation in response to acetylcholine (ACh), and endothelium-independent vasodilation in response to sodium nitroprusside (SNP; 17, 19, 20). Each of these responses was recorded following precontraction with phenylephrine (PE; 10^{-6} – 10^{-4} M, Sigma-Aldrich, St. Louis, MO) to ~70% of the maximal PE response (20). First, flow-induced shear stress was used to assess the endothelium-dependent vasodilatory response. Height of the fluid reservoirs was adjusted to achieve a pressure difference of 30 mmHg, which produced an approximate flow rate of $30 \mu\text{L} \cdot \text{min}^{-1}$ (20). Second, we assessed endothelium-dependent vasodilation in response to ACh. An ACh dose-response curve (ACh, 10^{-7} – 10^{-3} M, Sigma-Aldrich) was then performed. Last, maximal SNP-mediated endothelium-independent vasodilation was assessed by using a maximal dose of SNP (SNP, 10^{-3} M, Sigma-Aldrich). The same vessel from each participant ($n = 10$ PAD, $n = 11$ Con) was used for the entirety of the vessel experiments (flow, ACh, and SNP).

To account for baseline differences in vessel diameter for each experiment (i.e., flow, ACh, and SNP), vasodilation (%) was calculated as $(D_S - D_P / D_I - D_P) \times 100$, where D_S is the lumen diameter following the respective stimulus (flow, ACh, and SNP), D_P is the lumen diameter following precontraction with PE before each experiment, and D_I is the lumen diameter immediately before addition of PE (baseline diameter; 18, 20).

Mitochondrial Respiration

Skeletal muscle samples were stored in BIOPS for < 30 min before starting the fiber permeabilization procedures (21). Briefly, to facilitate optimal membrane permeability to substrates, skeletal muscle tissues were teased apart using needle-tip surgical forceps after the removal of adipose and connective tissues (21). Samples were placed in BIOPS with saponin stock (5 mg/mL) and were gently rocked for 30 min. Samples were rinsed twice in mitochondrial respiration medium [MiR05, containing (in mM) 0.5 EGTA, 3 $\text{MgCl}_2 \cdot 6\text{H}_2\text{O}$, 20

taurine, 10 KH₂-PO₄, 20 HEPES, 1 g/L BSA, 60 potassium-lactobionate, 110 sucrose, pH 7.1] for 10 min.

Mitochondrial respiratory O₂ flux was assessed using a high-resolution Oxygraph-2k (Oroboros, Innsbruck, Austria), as previously described (21). Briefly, permeabilized samples were weighed (~4–5 mg) using a standard analytical balance and were placed in the respirometer with 2 mL MiR05. Samples were constantly stirred at 37°C, and respiratory substrates and inhibitors (Table 1) were added. Baseline respiration was recorded before substrate administration. O₂ consumption of individual mitochondrial complexes was assessed by adding several respiratory substrates and inhibitors in the following order with the final concentrations in the chamber: glutamate-malate (2:10 mM), adenosine diphosphate (ADP; 5 mM), succinate (10 mM), cytochrome c (10 μM), rotenone (0.5 μM), antimycin-A (2.5 μM), oligomycin (5 mM), and *N,N,N,N*-tetramethyl-phenylenediamine (TMPD)-ascorbate (2:0.5 mM). Therefore, mitochondrial complexes were assessed: 1) complex I (CI) state 3 respiration, the ADP-activated state of oxidative phosphorylation assessed with the addition of glutamate + malate and ADP; 2) complex I + II (CI + II) state 3 respiration, assessed with the addition of glutamate + malate, ADP, and succinate; 3) complex II (CII) state 3 respiration, assessed with the addition of glutamate + malate, ADP, succinate, and rotenone; 4) mitochondrial membrane integrity, assessed with the addition of cytochrome c; 5) state 4 respiration, assessed by blocking ATP synthase with oligomycin; and 6) complex IV (CIV) respiration. It should be noted that autooxidation can increase residual oxygen consumption, therefore we determined the amount of oxygen consumption due to autooxidation of ascorbate + TMPD. After measuring CIV, CIV respiration was blocked by adding sodium azide to measure chemical respiration (21). Chemical respiration was subtracted from the total CIV respiration to calculate the reported CIV respiration (21). For each addition of substrate or inhibitor, the respiration rate was recorded after a stable response was achieved (~3–5 min). The O₂ consumption rate was measured as picomoles of O₂ per second and then calculated relative to the skeletal muscle sample mass (pmol·mg⁻¹·s⁻¹). The

respiratory control ratio (RCR), an index of the net oxidative coupling rate and ATP production efficiency, was calculated by the ratio of state 3/state 4 respiration (19, 20).

Citrate Synthase Activity

Citrate synthase activity was assessed to estimate mitochondrial content in the skeletal muscle samples, as previously described by Picard et al. (22). Briefly, skeletal muscle samples (frozen, ~2 to 3 mg dry wt) were homogenized using homogenization buffer (250 mM sucrose, 40 mM KCl, 2 mM EGTA, and 20 mM Tris HCl). Triton X-100 (0.1%) was added to the homogenate and was incubated for 60 min on ice. Samples were centrifuged for 8 min (10,000 *g*). The activity assay was read using a spectrophotometer (BioTek Instruments, Winooski, VT).

Table 1. *Mitochondrial respiration protocol*

Step	Substrate or Inhibitor	Complex Activity	Respiration State
1	Malate (2 mM) + glutamate (10 mM)	+ Complex I	Complex I state 2
2	ADP (5 mM)	+ Complex V	Complex I state 3
3	Succinate (10 mM)	+ Complex II	Complex I + II state 3
4	Rotenone (0.5 μ M)	-Complex I	Complex II state 3
5	Cytochrome-c (10 μ M)	Mitochondrial membrane integrity	
6	Oligomycin (5 mM)	-Complex V	State 4
7	Sodium azide (4 M) + ascorbate (0.5 mM) + TMPD (2 mM)	-Cytochrome-c oxidase + complex IV	Complex IV respiration

The site of action for the added chemicals to the respirometer included substrates (+) or inhibitors (-), and the respiration state was assessed for each step, respectively. ADP, adenosine diphosphate; TMPD, *N,N,N,N*-tetramethyl-phenylenediamine.

Immunoblotting

The relative abundance of proteins was assessed by standard Western blotting techniques in the skeletal muscle, according to manufacturer instructions using protocols as previously described (23). Briefly, protein was extracted from both PAD and Con skeletal muscle samples using a lysis buffer consisting of radio-immunoprecipitation assay buffer (RIPA; No. BP-115, Boston BioProducts, Ashland, MA) and 100x protease inhibitor (No. P8340, Sigma-Aldrich). A ratio of 200 μ L lysis buffer per 0.01 g of tissue was used to ensure equal loading. The

protein lysate was briefly vortexed and left on ice for 30 min. Samples were then centrifuged at 10,000 g at 4°C for 10 min. The supernatant was collected, and protein concentration was quantified using a Pierce BCA protein assay kit (No. 23225, Thermo Fisher Scientific, Waltham, MA). For the blots, 30 µL of loading sample containing 25 µg protein was warmed to 37°C for 10 min and loaded into a 15-well 12% polyacrylamide gel for electrophoresis and then transferred onto either a PVDF or nitrocellulose membrane overnight at 20 V in 4°C (No. 162-0260, Bio-Rad, Hercules, CA). Membranes were incubated in 5% nonfat dry milk (No. 170-6404, Bio-Rad) in Tris-buffered saline (TBS) at room temperature for 1 h. Membranes were incubated overnight at 4°C with primary antibodies: total OXPHOS (No. ab110413, 1:200, Abcam, Cambridge, MA), 4-hydroxynonenal (4-HNE, 1:2,000, No. ab46545, Abcam), and glutathione peroxidase-4 (GPX-4, 1:2,000, No. ab125066, Abcam). After washing membranes (5 min, 3 times), we incubated the membranes with anti-mouse IgG-HRP (No. 7076, Cell Signaling Technology, Danvers, MA) at a dilution of 1:2,000 for 1.5 h at room temperature, then washed again (10 min, 3 times). The membranes were developed in a chemiluminescence substrate (No. 170-5061, Bio-Rad). Image Lab software (v.4.1, Bio-Rad) was used for the densitometric analyses.

Skeletal Muscle Microvascular Oxygen Delivery and Utilization Capacity in Vivo

Continuous-wave near-infrared spectroscopy (NIRS) was used to noninvasively assess skeletal muscle microvascular oxygen delivery and utilization capacity at rest, during walking, and during recovery (tissue oxygenation index, TOI) using the Gardner-Skinner protocol (24). The portable NIRS device (PortaMon, Artinis, Einsteinweg, The Netherlands) with Oxysoft software (v. 3.0.103.3, Artinis) was adhered to the medial gastrocnemius with a commercially available adhesive and was wrapped in black cloth to block extraneous light from disturbing the signals (12, 25). Data were continuously collected at 1 Hz and were exported as Excel files for later analyses in MATLAB (v. R2021a, MathWorks, Natick, MA). The NIRS data were analyzed according to a modified Beer–Lambert’s law (26), as previously described (27). Briefly, the

walking protocol was used as an active hyper-emic stimulus to desaturate the skeletal muscle tissue. The TOI recovery rate, which represents the capacity by which the microcirculation can resaturate the tissue to the initial resting TOI values (27–29), was calculated using a linear regression model (from the end of exercise to the initial resting TOI values, $\% \cdot s^{-1}$; 27, 29). TOI minimum during walking and TOI maximum after recovery were normalized to baseline TOI values (expressed as a percentage of baseline TOI) (13).

Statistical Analysis

All statistical analyses were performed with GraphPad Prism v. 9.0.2 (GraphPad Software, San Diego, CA). Data normality was tested using the Shapiro–Wilk’s test. For descriptive characteristics, independent *t* tests were used for comparisons between Con and PAD groups. Fisher’s exact test was used for categorical variables (comorbidities and medications). Vasomotor function assessments were analyzed with a two-way repeated measures ANOVA. If significance was noted, Tukey’s test was used for post hoc comparisons. Flow, skeletal muscle mitochondrial respiration, citrate synthase activity, protein expression data, and in vivo skeletal muscle microvascular oxygenation data were analyzed using independent *t* tests. Nonparametric tests (i.e., Mann–Whitney tests and Kruskal–Wallis tests) were used for nonnormally distributed variables. Pearson’s product-moment correlation was used to assess the correlation between variables. Cohen’s *d* was performed to assess effect sizes and was interpreted as 0.2, 0.5, and 0.8 as small, moderate, and large effect sizes, respectively (12, 25, 30). A *P* value of <0.05 was considered significant for all analyses. All data are presented as means \pm SD.

RESULTS

Participant Characteristics

The Con group presented with greater ABI ($P < 0.01$) compared with the PAD group (Table 2), and patients with PAD had an average time from diagnosis of 5.6 ± 3.9 yr with stable symptoms. There were no statistical differences in

age, height, body mass, BMI, comorbidities, or medications between groups ($P > 0.05$; Table 2). Participants in both groups presented with several comorbidities and were regularly taking medications for these specific diseases and conditions (Table 2). Harvested vessel diameters following pressurization to 60 mmHg were not different between the Con and PAD groups (Con: $238.4 \pm 32.2 \mu\text{m}$, PAD: $207.5 \pm 37.4 \mu\text{m}$; $P = 0.34$). In addition, the vessel diameters for each experiment (i.e., flow, ACh, and SNP) were not statistically different within or between groups at baseline ($P = 0.18$) or following precontraction ($P = 0.98$).

Microvascular Function

All vessels for both PAD ($n = 10$) and Con ($n = 11$) were used in the final analyses for microvascular function. Endothelium-dependent vasodilatory function induced by flow was lower in PAD compared with Con (Con: $46.6 \pm 20.1\%$, PAD: $29.3 \pm 10.5\%$, $P = 0.03$; Fig. 1A). Furthermore, PAD arterioles demonstrated attenuated vasodilation in response to several ACh concentrations compared with Con at 10^{-4} M (Con: $58.5 \pm 9.5\%$, PAD: $39.4 \pm 18.6\%$, $P = 0.02$) and 10^{-3} M (Con: $71.1 \pm 11.1\%$, PAD: $45.7 \pm 18.1\%$, $P < 0.01$; Fig. 1B). On the contrary, endothelium-independent vasodilatory response induced by a maximal dose of SNP was not different between patients with PAD compared with Con (10^{-3} M, Con: $100.5 \pm 2.1\%$, PAD: $94.6 \pm 6.3\%$, $P = 0.30$; Fig. 1B).

Mitochondrial Respiratory Function and Citrate Synthase Activity

State 3 respiratory function was attenuated in PAD compared with Con for CI (Con: 12.4 ± 6.1 , PAD: $4.4 \pm 2.5 \text{ pmol}\cdot\text{s}^{-1}\cdot\text{mg}^{-1}$, $P < 0.01$), CI + II (Con: 27.4 ± 6.4 , PAD: $7.3 \pm 5.2 \text{ pmol}\cdot\text{s}^{-1}\cdot\text{mg}^{-1}$, $P < 0.01$), and CII (Con: 13.0 ± 10.3 , PAD: $3.2 \pm 3.1 \text{ pmol}\cdot\text{s}^{-1}\cdot\text{mg}^{-1}$, $P < 0.01$; Fig. 2A). State 4 respiration, an indicator of nonphosphorylating respiration, was not different between Con and PAD (Con: 4.7 ± 1.5 , PAD: $5.4 \pm 4.9 \text{ pmol}\cdot\text{s}^{-1}\cdot\text{mg}^{-1}$, $P = 0.59$), and CIV respiration was not different between groups (Con: 102.8 ± 31.1 , PAD: $83.9 \pm 36.2 \text{ pmol}\cdot\text{s}^{-1}\cdot\text{mg}^{-1}$, $P = 0.21$; Fig. 2A). RCR was greater in Con compared with PAD (Con: 5.3 ± 2.2 , PAD: 2.3 ± 1.9 , $P < 0.01$; Fig. 2B), and citrate synthase activity was

higher in PAD compared with Con (Con: 0.185 ± 0.01 , PAD: 0.200 ± 0.01 U·min⁻¹·μg⁻¹, $P = 0.02$).

Table 2. Participant characteristics for the control and patients with PAD

	Control	PAD	P Value
Participant characteristics			
<i>n</i>	11	10	
Age, yr	64 ± 8	68 ± 9	0.18
Height, cm	181.8 ± 9.9	174.2 ± 8.2	0.10
Mass, kg	94.1 ± 19.3	76.5 ± 20.5	0.07
Body mass index, kg/m ²	28.4 ± 4.8	24.8 ± 5.3	0.14
ABI	1.1 ± 0.1	0.6 ± 0.2†	<0.01
Walking distance (6 min), m	394.8 ± 55.7	252.7 ± 20.7†	<0.01
Risk factors and comorbidities, <i>n</i>			
Family history	7	4	0.2
Coronary artery disease	4	3	>0.99
Hypertension	4	5	0.67
Obesity	2	2	>0.99
Dyslipidemia	6	5	>0.99
Current smoker	2	5	0.18
Past smoker	4	3	>0.99
Cancer	2	0	0.48
Prediabetes	2	0	0.48
Diabetes mellitus	2	4	0.36
Renal disease	2	2	>0.99
COPD or lung disease	5	4	>0.99
Osteoporosis/arthritis	0	1	0.48
Medications, <i>n</i>			
Statins	6	6	>0.99
B-Blockers	1	5	0.06
Proton pump inhibitors	2	0	0.48
Anticoagulants	1	2	0.59
Diabetic therapy	3	4	0.66
Pin medication	3	1	0.59
Bronchodilators	4	1	0.31

Values are means ± SD or *n*. ABI, ankle-brachial index; COPD, chronic obstructive pulmonary disease; PAD, peripheral artery disease. † $P < 0.01$ vs. Con.

Protein Expression

Expression of 4-HNE, a marker of oxidative stress (31), was not different between patients with PAD and Con [Con: 0.08 ± 0.03 , PAD: 0.11 ± 0.01 arbitrary units (AU), $P = 0.06$; Fig. 3A], whereas GPX-4, an antioxidant marker (32), was lower in patients with PAD (Con: 0.24 ± 0.06 , PAD: 0.11 ± 0.04 AU, $P < 0.01$; Fig. 3B). In addition, the ratio between 4-HNE and GPX-4 was greater in patients with PAD (Con: 0.34 ± 0.06 , PAD: 1.14 ± 0.4 , $P < 0.01$; Fig. 3C). Furthermore, mitochondrial respiratory complex protein was lower in patients

with PAD compared with Con at CI (Con: 0.31 ± 0.08 , PAD: 0.16 ± 0.05 AU, $P < 0.01$), CII (Con: 0.44 ± 0.05 , PAD: 0.28 ± 0.04 AU, $P < 0.01$), CIII (Con: 0.29 ± 0.06 , PAD: 0.18 ± 0.06 AU, $P = 0.02$), CIV (Con: 0.25 ± 0.05 , PAD: 0.16 ± 0.03 AU, $P < 0.01$), and CV (Con: 0.34 ± 0.08 , PAD: 0.18 ± 0.09 AU, $P < 0.01$; Fig. 3D).

Relationships between Microvascular Function and Skeletal Muscle Mitochondrial Function

Assessments of flow-mediated vasodilation and ACh-mediated vasodilation in the skeletal muscle arterioles revealed significant relationships with skeletal muscle oxidative phosphorylating respiration. Flow-mediated vasodilation was positively associated with CI + II state 3 respiration ($r = 0.5$, $P = 0.03$; Fig. 4A), and ACh-mediated vasodilation exhibited a positive relationship with CI + II state 3 respiration ($r = 0.5$, $P = 0.02$; Fig. 4B). In addition, ACh-mediated vasodilation showed a positive relationship with RCR ($r = 0.5$, $P = 0.04$; Fig. 4C).

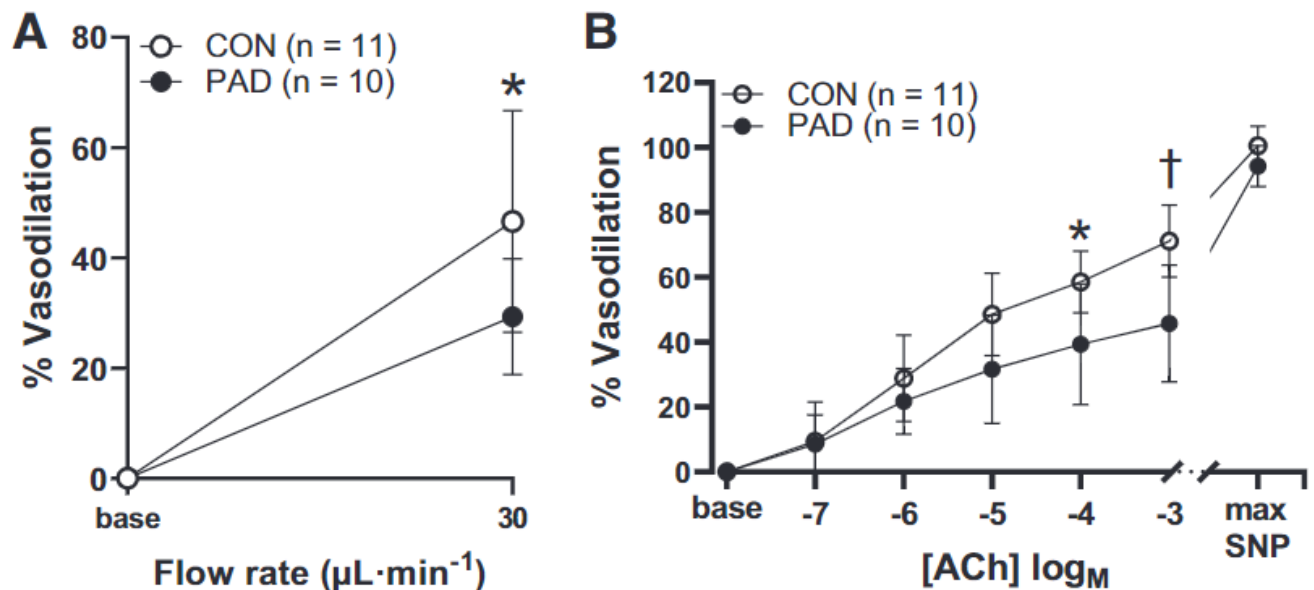


Figure 1. The vasomotor function of skeletal muscle arterioles from healthy controls (Con, $n = 11$) and patients with peripheral artery disease (PAD, $n = 10$) in response to flow ($30 \mu\text{L}\cdot\text{min}^{-1}$), acetylcholine (ACh, 10^{-7} – 10^{-3}), and sodium nitroprusside (SNP, 10^{-3}). **A:** flow-mediated vasodilatory response (%) was attenuated ($P = 0.03$) in PAD compared with Con. **B:** ACh-mediated vasodilatory response (%; 10^{-7} M to 10^{-3} M) was attenuated at 10^{-4} M ($P = 0.02$) and 10^{-3} M ($P < 0.01$) in PAD compared with Con. Maximal SNP-mediated vasodilatory response (%; 10^{-3} M) was not different ($P = 0.30$) between patients with PAD and Con. Data are means \pm SD. * $P < 0.05$ vs. Con. † $P < 0.01$ vs. Con.

Skeletal Muscle Microvascular Oxygen Delivery and Utilization Capacity, and Relationships between Ex Vivo Microvascular Function and Skeletal Muscle Oxidative Phosphorylating Respiration

The slope of TOI recovery after walking, an index of skeletal muscle microvascular oxygen delivery and utilization capacity (33, 34), was attenuated in patients with PAD compared with Con (Con: 0.51 ± 0.4 , PAD: $0.09 \pm 0.06\% \cdot s^{-1}$, $P = 0.04$; Fig. 5A). There were also no differences in baseline TOI (Con: $58.5 \pm 6.9\%$, PAD: $53.8 \pm 10.8\%$, $P = 0.42$), TOI minimum during walking (Con: $52.0 \pm 38.9\%$, PAD: $30.2 \pm 34.6\%$, $P = 0.35$), or maximum TOI after walking recovery (Con: $194.8 \pm 124.3\%$, PAD: $133.0 \pm 28.7\%$, $P = 0.26$). The slope of TOI recovery rate was positively associated with vasodilation to flow ($r = 0.8$, $P < 0.01$) and showed a positive albeit statistically insignificant relationship with maximal ACh-mediated vasodilation ($r = 0.5$, $P = 0.10$; Fig. 5, B and C). In addition, the slope of TOI recovery rate was positively associated with CI + II state 3 respiration ($r = 0.7$, $P = 0.03$; Fig. 5D). However, ABI, the clinical diagnostic assessment for PAD, demonstrated no distinct relationships with ACh-mediated vasodilation ($r = -0.3$, $P = 0.47$), flow-mediated vasodilation ($r = -0.3$, $P = 0.76$), or CI + II state 3 respiration ($r = -0.1$, $P = 0.88$) in PAD.

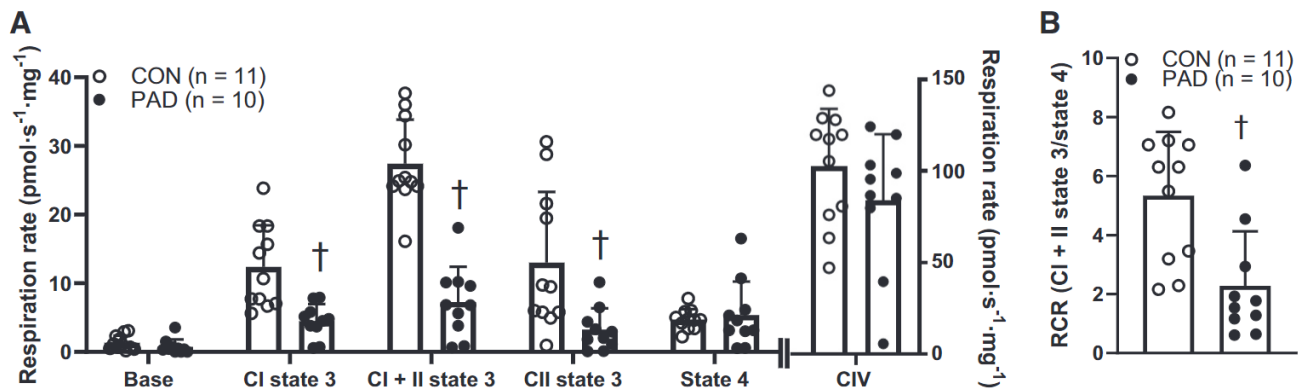


Figure 2. Skeletal muscle mitochondrial respiratory function from healthy controls (Con, $n = 11$) and patients with peripheral artery disease (PAD, $n = 10$). **A**: state 3 respiratory function ($\text{pmol} \cdot \text{s}^{-1} \cdot \text{mg}^{-1}$) was attenuated in PAD compared with Con at complex I (CI, $P < 0.01$), complex I + II (CI + II, $P < 0.01$), and complex II (CII, $P < 0.01$). State 4 respiration and complex IV (CIV) respiration ($\text{pmol} \cdot \text{s}^{-1} \cdot \text{mg}^{-1}$) were not different between Con and PAD ($P = 0.59$ and 0.21 , respectively). **B**: respiratory control ratio (RCR, CI + II state 3/state 4 respiration) was lower in PAD compared with Con ($P < 0.01$). Data are means \pm SD. † $P < 0.01$ vs. Con.

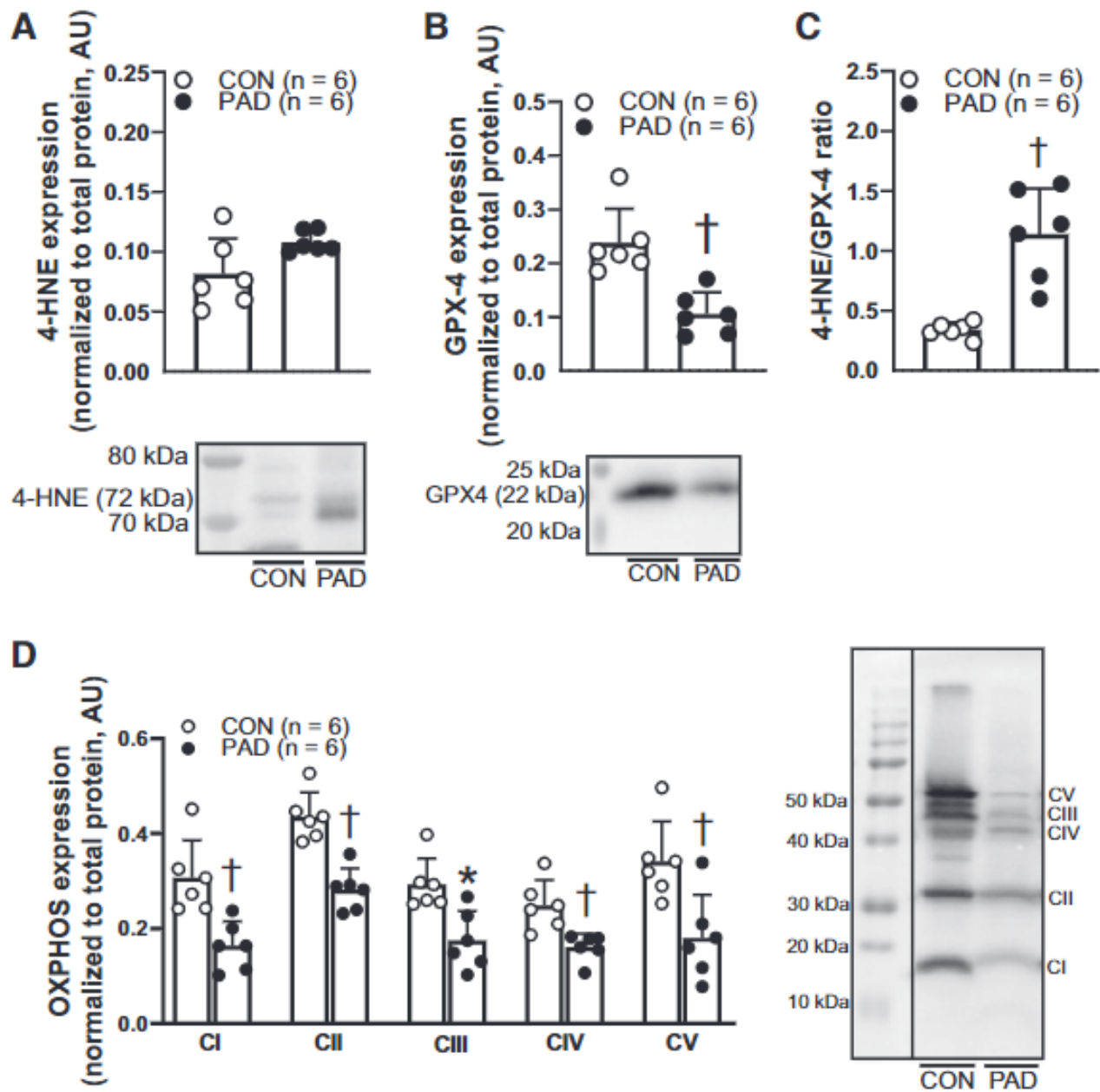


Figure 3. The expression of 4-hydroxynonenal (4-HNE), glutathione peroxidase 4 (GPX4), and electron transport chain proteins (total OXPHOS) in the skeletal muscle from healthy controls (Con, $n = 6$) and patients with peripheral artery disease (PAD, $n = 6$). Representative Western blot images consist of two continuous lanes (from the same blot) all normalized to total protein. **A**: 4-HNE expression was not different between Con and PAD groups ($P = 0.06$). **B**: GPX4 expression was lower in PAD compared with Con ($P < 0.01$). **C**: 4-HNE and GPX4 ratio, indicator of oxidative stress damage to antioxidant status, was attenuated in PAD compared with Con ($P < 0.01$). **D**: expression of proteins from the electron transport chain (complexes I–V, CI–V) was lower at CI ($P < 0.01$), CII ($P < 0.01$), CIII ($P = 0.02$), CIV ($P < 0.01$), and CV ($P < 0.01$) in PAD compared with Con.

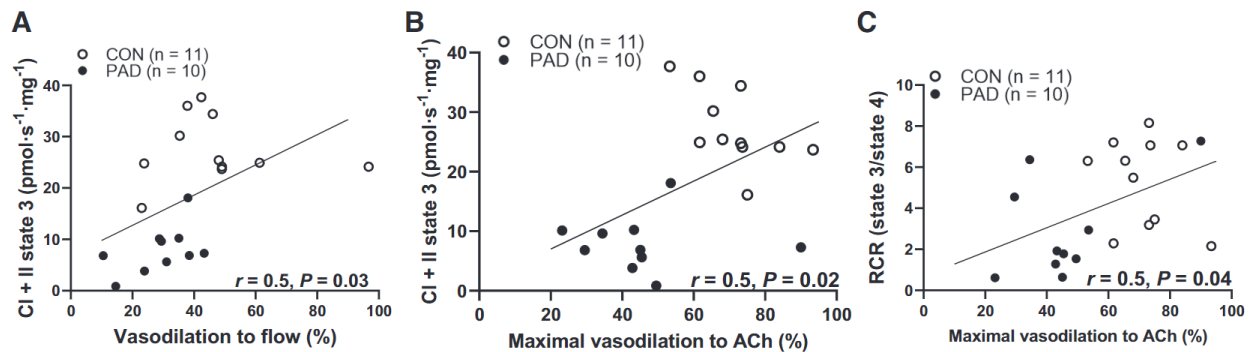


Figure 4. Relationships between vasodilatory capacity in response to flow ($30 \mu\text{L} \cdot \text{min}^{-1}$), acetylcholine (ACh, 10^{-3} M) with skeletal muscle oxidative phosphorylating respiration (CI + II state 3), respiratory control ratio (RCR) from healthy controls (Con, $n = 11$), and patients with peripheral artery disease (PAD, $n = 10$). *A*: positive relationship ($r = 0.5$, $P = 0.03$) between flow-mediated vasodilation (%) and complex I + II state 3 respiration ($\text{pmol} \cdot \text{s}^{-1} \cdot \text{mg}^{-1}$). *B*: positive relationship ($r = 0.5$, $P = 0.02$) between maximal ACh-mediated vasodilation (%) and complex I + II state 3 respiration ($\text{pmol} \cdot \text{s}^{-1} \cdot \text{mg}^{-1}$). *C*: positive relationship ($r = 0.5$, $P = 0.04$) between maximal ACh-mediated vasodilation (%) and RCR (state 3/state 4 respiration).

DISCUSSION

The presence of microvascular dysfunction in patients with PAD has been found to be strongly related to increased incidence of lower limb tissue loss (nonhealing ulcers and gangrene) and amputation (35–37). As expected, this has drawn increasing attention to the pathophysiology of the microvascular environment in patients with early-stage PAD with the aim of developing potential therapies that may aid in symptom management and in delaying, stopping, or even reversing disease progression. To our knowledge, we are the first group to directly examine skeletal muscle arteriole vasomotor function in PAD and to integrate ex vivo and in vivo findings regarding skeletal muscle mitochondrial function and microvascular oxygen delivery and utilization capacity in patients with PAD. This study produced several novel findings. First, we found that endothelium-dependent vasodilation was attenuated in the skeletal muscle arterioles of patients with PAD. Second, we found that attenuated endothelium-dependent vasodilation is moderately associated with reduced skeletal muscle mitochondrial function. In addition, we found that microvascular function is a stronger predictor of leg mitochondrial function and oxygen delivery and utilization capacity in the PAD legs than hemodynamic compromise (reflected in the ABI) produced by conduit artery blockages. Last, we evaluated the relationships between ex vivo skeletal muscle arteriole function and microvascular

function in vivo. Our findings indicate that in the calf skeletal muscle of claudicating patients with PAD, ex vivo arteriole endothelial function and myofiber mitochondrial respiration are related to in vivo skeletal muscle microvascular oxygen delivery and utilization capacity. Taken together, our results suggest that chronic leg ischemia, produced by atherosclerotic occlusive disease in the conduit arteries supplying the lower extremities, attenuates skeletal muscle arteriole endothelial function and this is likely an important contributor to the mitochondrial dysfunction and impaired microvascular oxygen delivery and utilization capacity in the skeletal muscle of the legs of claudicating patients with PAD. Notably, these findings suggest that therapies that target the microcirculation may delay or even reverse the progression of PAD.

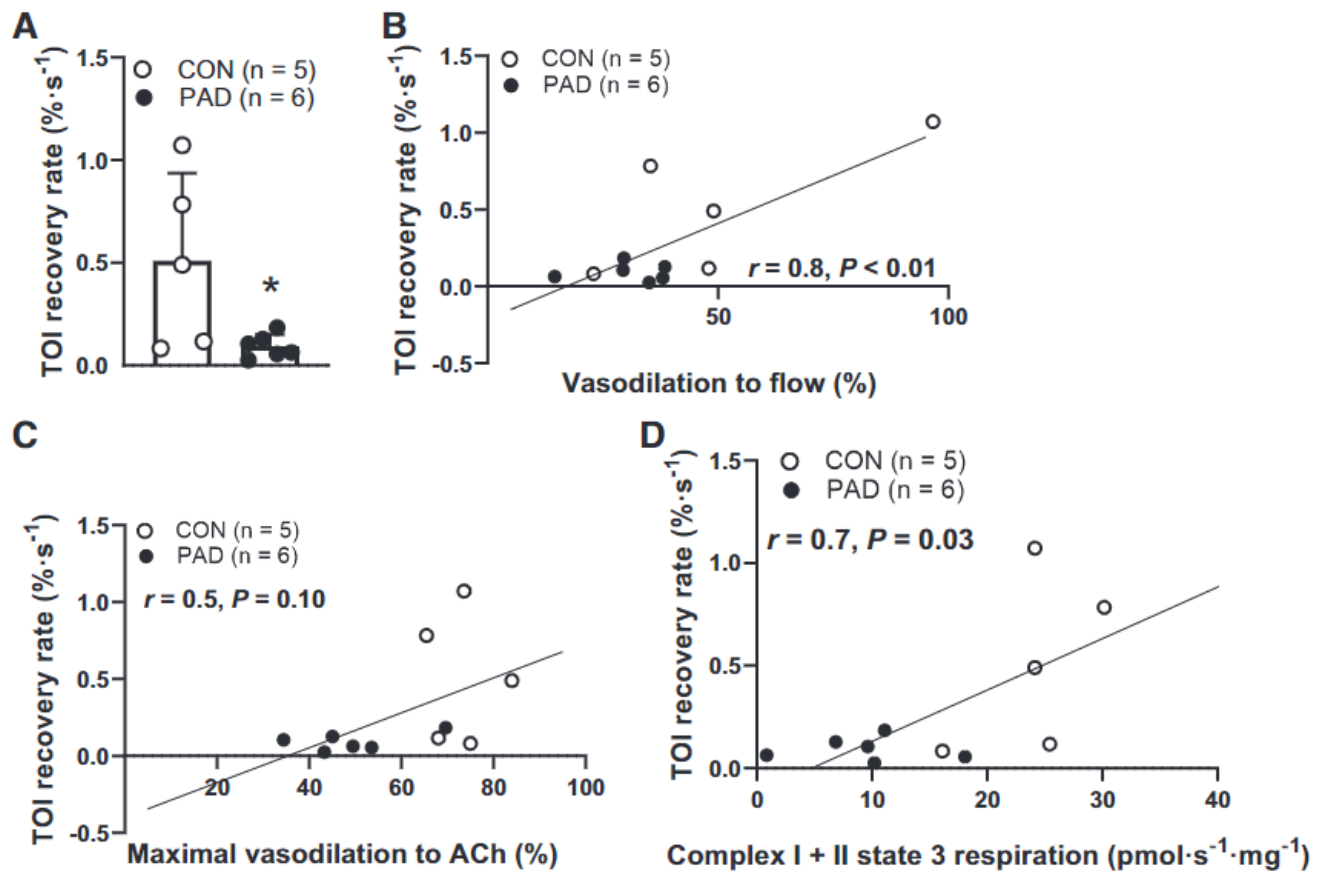


Figure 5. Measurements of in vivo skeletal muscle microvascular oxygenation capacity in healthy controls (Con, $n = 5$) and patients with peripheral artery disease (PAD, $n = 6$) for tissue oxygenation index (TOI) and relationships with flow-mediated vasodilation ($30 \mu\text{L} \cdot \text{min}^{-1}$), acetylcholine (ACh)-mediated dilation (10^{-3}M), and skeletal muscle oxidative phosphorylating respiration (CI + II state 3 respiration). **A**: the slope of TOI recovery ($\% \cdot \text{s}^{-1}$) was attenuated in PAD compared with Con ($P = 0.04$). **B**: positive relationship ($r = 0.8, P < 0.01$) between flow-mediated vasodilation (%) and slope of TOI recovery rate ($\% \cdot \text{s}^{-1}$). **C**: positive relationship ($r =$

0.5, $P = 0.10$) between maximal ACh-mediated vasodilation (%) and slope of TOI recovery rate ($\% \cdot s^{-1}$). *D*: positive relationship ($r = 0.7$, $P = 0.03$) between CI + II state 3 respiration ($\mu\text{mol} \cdot s^{-1} \cdot \text{mg}^{-1}$) and slope of TOI recovery rate ($\% \cdot s^{-1}$). Data are means \pm SD. * $P < 0.05$ vs. Con.

Microvascular Function

The flow-mediated dilation (FMD) technique is the most widely used noninvasive assessment of macrovascular endothelial function in healthy and disease populations. In brief, the procedure uses Doppler ultrasound to record the change in the diameter of a conduit artery (usually brachial or popliteal) in response to reactive hyperemia produced by cuff occlusion, and the response is calculated as a percent change from baseline arterial diameter (12, 25, 38). Using the FMD technique, we and others have reported that endothelial dysfunction is present in the conduit arteries of the upper and lower extremities of patients with PAD (12, 25, 39–41). However, very few studies have attempted to examine microvascular endothelial function in patients with PAD, probably due to the limited accessibility to human PAD tissues. The majority of these studies used in vivo approaches for the assessment of the microcirculation localized to the skin (42–45) and the muscle (46, 47). These methods have been rather heterogeneous and included techniques such as laser Doppler (42, 43), microdialysis (42–45), MRI (46, 47), and NIRS (48, 49). Fronck et al. (42, 43) assessed microvascular endothelial activity using ACh iontophoretic administration with laser Doppler flowmetry, and they found that endothelial activity is attenuated in patients with PAD compared with healthy individuals. Rossi et al. (44, 45) also reported blunted endothelial function in response to iontophoretic ACh administration in patients with PAD compared with controls. Others have demonstrated attenuated microvascular endothelial responsiveness to reactive hyperemia using MRI and described that attenuated endothelial function is related to the stage of PAD, with patients with CLI having worse function than patients with claudication (46, 47). Although these previous studies suggest that attenuated endothelium-dependent vasodilatory function is present in the PAD microcirculation, these techniques have limitations, such as lacking the ability to directly assess the skeletal muscle microcirculation (50). These

constraints may raise several issues with data interpretation, especially when considering that skin and muscle vascular beds have distinct hemodynamic control mechanisms (37).

To our knowledge, we are the first group to isolate and directly assess the skeletal muscle arteriole vasodilatory function from the legs of patients with PAD. Our results indicate that flow-mediated and ACh-mediated vasodilation, both indicators of endothelial function, are attenuated in PAD (Fig. 1, *A* and *B*). On the other hand, smooth muscle function assessed by SNP was not different between groups (Fig. 1*B*), which is consistent with our previous preliminary findings in the PAD microcirculation and the findings of others in the macrocirculation (12, 41). These findings suggest that PAD produces a state of impaired microvascular function that is more readily apparent at the level of the arterial intima and endothelium than that of the arterial media and vascular smooth muscle (51). It is important to consider that this attenuation in microvascular endothelial function is presumably multifaceted with several mechanisms contributing to these deficits. First, ischemia alone has been shown to increase ROS production within skeletal muscle arterioles (9), which may induce oxidative stress and damage that can attenuate microvascular function. Second, PAD is often characterized by frequent cycles of ischemia-reperfusion, occurring every time a patient with PAD walks (52, 53). Several studies have demonstrated that ischemia-reperfusion within the skeletal muscle microcirculation can facilitate excessive ROS production, leukocyte activation, and inflammation, which jointly contribute to increased micro-vascular permeability, endothelial dysfunction, and micro-vascular injury (10, 54–59). Collectively, these mechanisms may impair hemodynamic regulation and increase peripheral vascular resistance, thus altering tissue perfusion that may lead to skeletal muscle damage (7, 8). Of note, our results show that patients with PAD demonstrate a trend for greater levels of intramuscular 4-HNE (Fig. 3*A*) and lower expression of GPX-4 (Fig. 3*B*). These results are consistent with previous research that indicated increased oxidative stress damage and attenuated antioxidant markers in the PAD skeletal muscle (7, 8, 60).

Furthermore, we found that the 4-HNE-to-GPX-4 ratio is greater in patients with PAD compared with Con (Fig. 3C), which further confirms that an imbalance between oxidative stress and antioxidant defense mechanisms persists in the PAD skeletal muscle environment.

Skeletal Muscle Mitochondrial Function

Several previous studies reported on the components of the skeletal muscle mitochondrial dysfunction present in PAD (61), such as dysfunctional electron transport chain, reduced ATP production, damaged ultrastructure and DNA, and impaired antioxidant enzyme activity (7, 62–67). With the permeabilized fiber method, it has been shown that patients with PAD have impaired mitochondrial respiratory function at CI, CIII, and CIV (7, 62, 63). The data from the present study confirm and build upon these previous findings, as we found that CI state 3, CI + II state 3, and CII state 3 respiration are attenuated in patients with PAD (Fig. 2A). In addition, RCR, which has been identified as an indicator of net oxidative coupling rate and ATP production efficiency (20), was lower in patients with PAD (Fig. 2B). In further support of this mitochondrial dysfunction, we also found decreased protein expression of the mitochondrial electron transport chain complexes (Fig. 3D). The decreased mitochondrial respiratory complex protein expression may be one of the mechanisms operating to produce reduced oxygen consumption and ATP production coupling in PAD, which coincides with our findings regarding mitochondrial respiratory function and ATP production efficiency (RCR). These data support that a dysfunctional bioenergetic environment prevails in the PAD skeletal muscle, which likely further exacerbates the well-known blood flow limitations and oxidative stress produced by the blocked conduit arteries in the legs of patients with PAD (62, 68).

We and others have used citrate synthase activity in humans and animal models (19, 21, 63, 69), which is recognized as a sound assessment of skeletal muscle mitochondrial content (70). In chronically ischemic skeletal muscle, it has been suggested that mitochondrial content increases to compensate for the

dysfunctional bioenergetic environment (63). In the present study, we found that patients with PAD have greater citrate synthase activity compared with controls (Con: $0.185 \pm 0.01 \text{ U} \cdot \text{min}^{-1} \cdot \mu\text{g}^{-1}$, PAD: $0.200 \pm 0.01 \text{ U} \cdot \text{min}^{-1} \cdot \mu\text{g}^{-1}$, $P = 0.02$), which is consistent with previous work in human PAD and mouse models for citrate synthase activity (63, 69). These data may provide additional evidence to support that increased mitochondrial content may be a potential compensatory mechanism for the bioenergetic impairments in the PAD skeletal muscle. However, the increased citrate synthase activity does not appear to be sufficient to satisfy the bioenergetic demands of the affected muscles, as respiration per mitochondrion and ATP production efficiency (RCR) are compromised in PAD.

Microvascular Function and Skeletal Muscle Mitochondrial Function

Although skeletal muscle mitochondrial dysfunction in PAD has been well documented (7, 63), little work has been done to identify the mechanisms underlying these deficits. In the present study, we sought to investigate microvascular endothelial dysfunction as a contributing mechanism to skeletal muscle mitochondrial dysfunction. Our data demonstrate that skeletal muscle arteriole flow-mediated vasodilation and ACh-mediated vasodilation are both positively associated with oxidative phosphorylation capacity in the skeletal muscle (Fig. 4, A and B), and ACh-mediated vasodilation is also positively associated with RCR (Fig. 4C). These correlations between skeletal muscle arteriole endothelial function and skeletal muscle mitochondrial function may be interpreted as moderate-strength positive relationships; however, in conjunction with effect size analyses, these correlations may be more meaningful. Cohen's d revealed that these variables have large effect sizes (flow: $d = 1.1$, ACh 10^{-3} M : $d = 1.7$, complex I + II state 3 respiration: $d = 3.4$, and RCR: $d = 1.5$), which further support the clinical relevance of these relationships.

Our findings indicate that the microcirculation, specifically skeletal muscle arteriole endothelial dysfunction, may be an important contributor to the mitochondrial myopathy of PAD (61, 71–73). Previous work has suggested that the microcirculation is critical for hemodynamic regulation, perfusion, and oxygen

extraction within the skeletal muscle, especially when oxygen supply is limited (4–6, 74). These ischemic conditions can be particularly harmful for the skeletal muscle mitochondrial environment and can subsequently result in bioenergetic deficiencies, impaired enzymatic activity, and augmented ROS production (68, 75), which ultimately facilitates a deleterious environment that generates skeletal muscle mitochondrial dysfunction and oxidative damage (7, 63, 76). In addition, this detrimental environment that is local to the ischemic tissue may adversely impact the vessels that perfuse it, thus impacting the systemic circulation (77, 78). These elevated levels of circulating ROS may generate a vicious cycle that impairs systemic vascular function in patients with PAD, but the exact mechanisms underlying these relationships and potential causal roles of endothelial dysfunction warrant further investigation (77, 78).

Ex Vivo Microvascular Function and in Vivo Skeletal Muscle Microvascular Oxygen Delivery and Utilization Capacity

To further explore whether our ex vivo findings of microvascular function can be translated to the in vivo skeletal muscle microcirculation, we assessed skeletal muscle microvascular oxygen delivery and utilization capacity in vivo using NIRS. To adequately assess the skeletal muscle microcirculation noninvasively, it has been suggested that a hyperemic stimulus (i.e., exercise or cuff occlusion) should be used in addition to assessing resting values (50). We and others have successfully used exercise as a hyperemic stimulus to assess calf muscle tissue oxygen delivery and utilization in patients with PAD (11–13, 25, 28). We noted that basal TOI (Con: $58.5 \pm 6.9\%$, PAD: $53.8 \pm 10.8\%$, $P = 0.42$) and the maximal TOI recovery after exercise were not different between groups (Con: $194.8 \pm 124.3\%$, PAD: $133.0 \pm 28.7\%$, $P = 0.26$). These data are consistent with previous work, as patients with PAD who have mild-to-moderate claudication have normal skeletal muscle tissue perfusion at rest and show no difference in their maximal level of recovery following walking exercise (13, 79). These works also demonstrated that patients with PAD experience a greater reduction in TOI during walking exercise compared with controls, which suggests

that patients with PAD experience a greater amount of tissue desaturation during activity (13, 79). Although we did not achieve statistical significance for this metric in the present study (Con: $52.0 \pm 38.9\%$, PAD: $30.2 \pm 34.6\%$, $P = 0.35$), we noted a moderate effect size ($d = 0.6$), which may suggest a clinical difference in the TOI minimum during walking between groups. Last and consistent with previous work (13, 79), we found that patients with PAD demonstrated a slower slope of TOI recovery compared with Con (Fig. 5A). This may indicate that patients with PAD have blunted skeletal muscle microvascular oxygen delivery capacity (33, 34) and may provide in vivo evidence of microcirculatory dysfunction in the PAD skeletal muscle.

We found that ex vivo flow-mediated vasodilation is positively associated with the slope of TOI recovery rate ($r = 0.8$, $P < 0.01$; Fig. 5B), whereas ACh-mediated vasodilation showed a trend to be positively associated with the slope of TOI recovery rate ($r = 0.5$, $P = 0.10$; Fig. 5C). Our effect size analyses (Cohen's d ; large effect sizes, TOI recovery rate: $d = 1.5$, flow: $d = 1.1$, and ACh 10^{-3} M: $d = 1.7$) support these moderate-positive correlations and suggest that the skeletal muscle microcirculatory endothelial function may play a role in calf muscle microvascular oxygen delivery and utilization capacity in vivo, and they may supply evidence that supports the roles of the skeletal muscle arterioles in regulating blood flow and oxygen transport in PAD (3). It may be possible that methods that enhance the endothelial function of the skeletal muscle microvessels in patients with PAD may improve blood flow and oxygen delivery and utilization capacity, which may be an area of interest for developing new and much-needed therapies to delay and/or possibly reverse the progression of PAD.

In addition, we noted that oxidative phosphorylation capacity (CI + II state 3 respiration) was positively associated with TOI recovery rate ($r = 0.7$, $P = 0.03$; Fig. 5D), and our effect size analyses also complement these relationships (complex I + II state 3 respiration: $d = 3.4$ and TOI recovery rate: $d = 1.5$). These data may support the notion that attenuated mitochondrial oxidative phosphorylation capacity at the level of the skeletal muscle may be a

consequence of poor skeletal muscle microvascular oxygen delivery and utilization capacity in patients with PAD. Although we have previously shown that improving macrovascular endothelial function with a mitochondrial-targeted therapy improves leg skeletal muscle function and walking performance in patients with PAD (27), the current results are the first to provide an integrated approach of directly investigating skeletal muscle arteriole endothelial function and skeletal muscle mitochondrial function in parallel with leg skeletal muscle microvascular oxygen transfer and utility capacity in vivo in claudicating patients with PAD. These integrative findings may be crucial for future work, as the microcirculation appears to be a promising potential predictor of leg function and a key target for novel therapies for patients with PAD.

Contribution of Microvascular and Skeletal Muscle Mitochondrial Dysfunction to PAD Manifestations

It has been previously shown that the ABI assessment reflecting occlusive disease in the conduit arteries supplying the lower extremities (macrovascular disease) cannot adequately explain the symptoms, walking impairment, and degree of myopathy in PAD (52, 53, 80). Our findings support this premise, as we found that ABI was weakly associated with ACh-mediated vasodilation ($r = -0.3$, $P = 0.47$), flow-mediated vasodilation ($r = -0.3$, $P = 0.76$), and skeletal muscle CI + II state 3 respiration ($r = -0.1$, $P = 0.88$) in claudicating PAD. On the contrary, we found that microcirculatory function may be stronger than ABI as a predictor of leg mitochondrial function and oxygen delivery and utilization capacity (Figs. 4 and 5), which further supports our hypothesis on the importance of the microcirculation as a key component of the pathophysiology of PAD. In addition, upon further analysis, we found a negative relationship between time from diagnosis and maximal ACh-mediated vasodilation ($r = -0.8$, $P = 0.04$), and negative albeit insignificant relationships between time from diagnosis and vasodilation to flow ($r = -0.5$, $P = 0.29$) and CI + II state 3 respiration ($r = -0.3$, $P = 0.54$). These relationships likely indicate the cumulative nature of the insult to the microcirculation and skeletal muscle mitochondria in PAD muscle,

resulting from chronic repetitive episodes of ischemia- reperfusion that occur every time a patient with claudication walks. Furthermore, the microvasculature exhibits a stronger relationship with disease duration when compared with mitochondrial respiration.

It is important to consider the temporal sequence and connection between microvascular and skeletal muscle mitochondrial dysfunction, the roles they play in PAD pathophysiology, and the generation of PAD manifestations. With this being the first time to directly investigate the skeletal muscle microcirculation in patients with PAD, it is difficult to draw definitive conclusions. Previous in vivo work in rodents has suggested that the skeletal muscle microcirculation is subject to ischemia-reperfusion damage before the skeletal muscle tissue is affected (10). Although preliminary, these correlations suggest that the microvascular endothelial dysfunction may precede skeletal muscle mitochondrial dysfunction, although both are produced by the chronic damage of repetitive episodes of ischemia-reperfusion as encountered during routine walking over the months and years that the occlusive disease is advancing in the leg arteries of patients with PAD. However, extensive investigation is still required to ascertain an answer to this perplexing question. Our previous work showed that acute oral mitochondrial-targeted antioxidant (Mito-Q, 80 mg) intake can improve vascular endothelial function and walking capacity in patients with claudicating PAD in vivo (12), and acute Mito-Q incubation can reverse age-related vascular dysfunction in human skeletal muscle feed arteries (17). Our group plans to perform similar investigations to determine potential differential mechanisms underlying both microvascular and skeletal muscle mitochondrial dysfunction in claudicating PAD.

Experimental Considerations

It is important to note that this study has some experimental considerations. First, our study participants were all males, and thus our findings may not be directly generalizable to female patients with PAD. Future studies should power for sex differences in the skeletal muscle microcirculation in

patients with PAD. Second, although the use of walking as a hyperemic stimulus for NIRS may be clinically applicable in patients with claudication, future work should use a more consistent method such as cuff occlusion to induce reactive hyperemia. In addition, NIRS may be sensitive to the severity and chronicity of PAD, and it will be important to attempt to identify and recruit patients with early-stage PAD so we can evaluate the earliest events in calf muscle ischemic damage and myopathy before the disease progresses to later stages. In addition, the participants were actively using medications, such as b-blockers, metformin, anticoagulants, and bronchodilators, which have may altered vascular reactivity properties or reduced inflammation. Furthermore, with human samples, we do not always get the same quantity of tissue per biopsy, and for this reason, our protein expression data have a lower sample size in comparison with our primary outcome assessments of microvascular and skeletal muscle mitochondrial function.

Conclusion and Future Direction

Our data demonstrate, for the first time, that skeletal muscle arteriole endothelium-mediated vasodilatory function is attenuated in patients with PAD. Our findings also identify an association between microcirculatory endothelial dysfunction and the skeletal muscle mitochondrial respiratory function. Last, we integrated our ex vivo findings with in vivo assessments of skeletal muscle microvascular oxygen delivery and utilization capacity and found that skeletal muscle arteriole endothelial function and skeletal muscle mitochondrial respiratory function are directly related to in vivo leg skeletal muscle microvascular oxygen delivery and utilization capacity in patients with PAD. Our work suggests that chronic leg ischemia produced by atherosclerotic blockages in conduit arteries of the legs attenuates skeletal muscle arteriole endothelial function, and this may be a principal mediator of mitochondrial dysfunction and impaired muscle oxygen delivery and utilization capacity in the affected legs of patients with PAD. Notably, the information from the present study suggests that microcirculatory endothelial dysfunction may be a key contributor in the

bioenergetic and oxygen transfer and utility deficits of the ischemic legs in PAD. This demonstrates the importance of microcirculatory endothelial dysfunction as a therapeutic target in the care of claudicating patients with PAD.

GRANTS

This work was supported by National Institutes of Health (NIH) COBRE Pilot Award P20GM109090, National Aeronautics and Space Administration Nebraska Space Grant NNX15AI09H, NIH Grants R01 AG034995 and R01 AG049868, and resources and the use of facilities at the Veterans Affairs Nebraska-Western Iowa Health Care System.

DISCLOSURES

No conflicts of interest, financial or otherwise, are declared by the authors.

AUTHOR CONTRIBUTIONS

S.-Y.P. and E.J.P. conceived and designed research; S.-Y.P., E.J.P., C.P.A., T.N.K., P.K.M., M.N.S., T.K.W., J.R.T., K.S.K., and I.I.P. performed experiments; S.-Y.P., E.J.P., C.P.A., and T.N.K. analyzed data; S.-Y.P. and E.J.P. interpreted results of experiments; E.J.P., C.P.A., and T.K.W. prepared figures; S.-Y.P. and E.J.P. drafted manuscript; S.-Y.P., E.J.P., and I.I.P. edited and revised manuscript; S.-Y.P., E.J.P., C.P.A., T.N.K., P.K.M., M.N.S., T.K.W., J.R.T., K.S.K., and I.I.P. approved final version of manuscript.

REFERENCES

1. Shu J, Santulli G. Update on peripheral artery disease: epidemiology and evidence-based facts. *Atherosclerosis* 275: 379–381, 2018.
doi:10.1016/j.atherosclerosis.2018.05.033.
2. Selvin E, Erlinger TP. Prevalence of and risk factors for peripheral arterial disease in the United States: results from the National Health and Nutrition Examination Survey, 1999-2000. *Circulation* 110: 738– 743, 2004.
doi:10.1161/01.CIR.0000137913.26087.F0.
3. Rahman M, Siddik AB. Anatomy, Arterioles. In: *StatPearls*. Treasure Island, FL: StatPearls Publishing, 2021.

4. Fronek K, Zweifach BW. Microvascular pressure distribution in skeletal muscle and the effect of vasodilation. *Am J Physiol* 228: 791– 796, 1975.
doi:10.1152/ajplegacy.1975.228.3.791.
5. Sweeney TE, Sarelius IH. Arteriolar control of capillary cell flow in striated muscle. *Circ Res* 64: 112–120, 1989. doi:10.1161/01.res.64.1.112.
6. Eriksson E, Lisander B. Changes in precapillary resistance in skeletal muscle vessels studied by intravital microscopy. *Acta Physiol Scand* 84: 295–305, 1972.
doi:10.1111/j.1748-1716.1972.tb05181.x.
7. Pipinos II, Judge AR, Zhu Z, Selsby JT, Swanson SA, Johannig JM, Baxter BT, Lynch TG, Dodd SL. Mitochondrial defects and oxidative damage in patients with peripheral arterial disease. *Free Radic Biol Med* 41: 262–269, 2006.
doi:10.1016/j.freeradbiomed.2006.04.003.
8. Weiss DJ, Casale GP, Koutakis P, Nella AA, Swanson SA, Zhu Z, Miserlis D, Johannig JM, Pipinos II. Oxidative damage and myofiber degeneration in the gastrocnemius of patients with peripheral arterial disease. *J Transl Med* 11: 230, 2013.
doi:10.1186/1479-5876-11-230.
9. Baudry N, Laemmel E, Vicaut E. In vivo reactive oxygen species production induced by ischemia in muscle arterioles of mice: involvement of xanthine oxidase and mitochondria. *Am J Physiol Heart Circ Physiol* 294: H821–H828, 2008.
doi:10.1152/ajpheart.00378.2007.
10. Pemberton M, Anderson G, Barker J. In vivo microscopy of microcirculatory injury in skeletal muscle following ischemia/reperfusion. *Microsurgery* 15: 374–382, 1994.
doi:10.1002/micr.1920150604.
11. Gardner AW, Montgomery PS, Wang M, Shen B. Association between calf muscle oxygen saturation with ambulatory function and quality of life in symptomatic patients with peripheral artery disease. *J Vasc Surg* 72: 632–642, 2020.
doi:10.1016/j.jvs.2019.09.057.
12. Park SY, Pekas EJ, Headid RJ 3rd, Son WM, Wooden TK, Song J, Layec G, Yadav SK, Mishra PK, Pipinos II. Acute mitochondrial antioxidant intake improves endothelial function, antioxidant enzyme activity, and exercise tolerance in patients with peripheral artery disease. *Am J Physiol Heart Circ Physiol* 319: H456–H467,

2020. doi:10.1152/ajpheart.00235.2020.

13. Fuglestad MA, Hernandez H, Gao Y, Ybay H, Schieber MN, Brunette KE, Myers SA, Casale GP, Pipinos II. A low-cost, wireless near-infrared spectroscopy device detects the presence of lower extremity atherosclerosis as measured by computed tomographic angiography and characterizes walking impairment in peripheral artery disease. *J Vasc Surg* 71: 946–957, 2020. doi:10.1016/j.jvs.2019.04.493.
14. McCamley JD, Cutler EL, Schmid KK, Wurdeman SR, Johanning JM, Pipinos II, Myers SA. Gait mechanics differences between healthy controls and patients with peripheral artery disease after adjusting for gait velocity stride length and step width. *J Appl Biomech* 35: 19–24, 2019. doi:10.1123/jab.2017-0257.
15. Schieber MN, Hasenkamp RM, Pipinos II, Johanning JM, Stergiou N, DeSpiegelaere HK, Chien JH, Myers SA. Muscle strength and control characteristics are altered by peripheral artery disease. *J Vasc Surg* 66: 178–186.e12, 2017. doi:10.1016/j.jvs.2017.01.051.
16. Myers SA, Applequist BC, Huisinga JM, Pipinos II, Johanning JM. Gait kinematics and kinetics are affected more by peripheral arterial disease than by age. *J Rehabil Res Dev* 53: 229–238, 2016. doi:10.1682/JRRD.2015.02.0027.
17. Park SY, Kwon OS, Andtbacka RHI, Hyingstrom JR, Reese V, Murphy MP, Richardson RS. Age-related endothelial dysfunction in human skeletal muscle feed arteries: the role of free radicals derived from mitochondria in the vasculature. *Acta Physiol* 222: e12893, 2018. doi:10.1111/apha.12893.
18. Park SY, Ives SJ, Gifford JR, Andtbacka RH, Hyingstrom JR, Reese V, Layec G, Bharath LP, Symons JD, Richardson RS. Impact of age on the vasodilatory function of human skeletal muscle feed arteries. *Am J Physiol Heart Circ Physiol* 310: H217–H225, 2016 [Erratum in *Am J Physiol Heart Circ Physiol* 312: H347, 2017] doi:10.1152/ajpheart.00716.2015.
19. Park SH, Kwon OS, Park SY, Weavil JC, Andtbacka RHI, Hyingstrom JR, Reese V, Richardson RS. Vascular mitochondrial respiratory function: the impact of advancing age. *Am J Physiol Heart Circ Physiol* 315: H1660–H1669, 2018. doi:10.1152/ajpheart.00324.2018.
20. Park SH, Kwon OS, Park SY, Weavil JC, Hydren JR, Reese V, Andtbacka RHI,

- Hyngstrom JR, Richardson RS. Vasodilatory and vascular mitochondrial respiratory function with advancing age: evidence of a free radically mediated link in the human vasculature. *Am J Physiol Regul Integr Comp Physiol* 318: R701–R711, 2020. doi:10.1152/ajpregu.00268.2019.
21. Park SY, Gifford JR, Andtbacka RHI, Trinity JD, Hyngstrom JR, Garten RS, Diakos NA, Ives SJ, Dela F, Larsen S, Drakos S, Richardson RS. Cardiac, skeletal, and smooth muscle mitochondrial respiration: are all mitochondria created equal? *Am J Physiol Heart Circ Physiol* 307: H346–H352, 2014. doi:10.1152/ajpheart.00227.2014.
 22. Picard M, Csukly K, Robillard ME, Godin R, Ascah A, Bourcier- Lucas C, Burelle Y. Resistance to Ca^{2+} -induced opening of the permeability transition pore differs in mitochondria from glycolytic and oxidative muscles. *Am J Physiol Regul Integr Comp Physiol* 295: R659–R668, 2008. doi:10.1152/ajpregu.90357.2008.
 23. Kambis TN, Shahshahan HR, Kar S, Yadav SK, Mishra PK. Transgenic expression of miR-133a in the diabetic akita heart prevents cardiac remodeling and cardiomyopathy. *Front Cardiovasc Med* 6: 45, 2019. doi:10.3389/fcvm.2019.00045.
 24. Gardner AW, Parker DE, Webb N, Montgomery PS, Scott KJ, Blevins SM. Calf muscle hemoglobin oxygen saturation characteristics and exercise performance in patients with intermittent claudication. *J Vasc Surg* 48: 644–649, 2008. doi:10.1016/j.jvs.2008.04.005.
 25. Pekas EJ, Wooden TK, Yadav SK, Park SY. Body mass-normalized moderate dose of dietary nitrate intake improves endothelial function and walking capacity in patients with peripheral artery disease. *Am J Physiol Regul Integr Comp Physiol* 321: R162–R173, 2021. doi:10.1152/ajpregu.00121.2021.
 26. Ferreira LF, Hueber DM, Barstow TJ. Effects of assuming constant optical scattering on measurements of muscle oxygenation by near-infrared spectroscopy during exercise. *J Appl Physiol (1985)* 102: 358–367, 2007. doi:10.1152/jappphysiol.00920.2005.
 27. Headid RJ 3rd, Pekas EJ, Wooden TK, Son WM, Layec G, Shin J, Park SY. Impacts of prolonged sitting with mild hypercapnia on vascular and autonomic function in healthy recreationally active adults. *Am J Physiol Heart Circ Physiol* 319: H468–H480, 2020. doi:10.1152/ajpheart.00354.2020.

28. Hart CR, Layec G, Trinity JD, Le Fur Y, Gifford JR, Clifton HL, Richardson RS. Oxygen availability and skeletal muscle oxidative capacity in patients with peripheral artery disease: implications from in vivo and in vitro assessments. *Am J Physiol Heart Circ Physiol* 315: H897–H909, 2018. doi:10.1152/ajpheart.00641.2017.
29. Park SY, Wooden TK, Pekas EJ, Anderson CP, Yadav SK, Slivka DR, Layec G. Effects of passive and active leg movements to interrupt sitting in mild hypercapnia on cardiovascular function in healthy adults. *J Appl Physiol (1985)* 132: 874–887, 2022. doi:10.1152/japplphysiol.00799.2021.
30. Sullivan GM, Feinn R. Using effect size-or why the P value is not enough. *J Grad Med Educ* 4: 279–282, 2012. doi:10.4300/JGME-D-12-00156.1.
31. Zarkovic N. 4-hydroxynonenal as a bioactive marker of pathophysiological processes. *Mol Aspects Med* 24: 281–291, 2003. doi:10.1016/ s0098-2997(03)00023-2.
32. Imai H, Nakagawa Y. Biological significance of phospholipid hydroperoxide glutathione peroxidase (PHGPx, GPx4) in mammalian cells. *Free Radic Biol Med* 34: 145–169, 2003. doi:10.1016/s0891-5849(02)01197-8.
33. Bopp CM, Townsend DK, Warren S, Barstow TJ. Relationship between brachial artery blood flow and total [hemoglobin + myo- globin] during post-occlusive reactive hyperemia. *Microvasc Res* 91: 37–43, 2014. doi:10.1016/j.mvr.2013.10.004.
34. Gayda M, Juneau M, Tardif JC, Harel F, Levesque S, Nigam A. Cardiometabolic and traditional cardiovascular risk factors and their potential impact on macrovascular and microvascular function: preliminary data. *Clin Hemorheol Microcirc* 59: 53–65, 2015. doi:10. 3233/CH-141816.
35. Beckman JA, Duncan MS, Damrauer SM, Wells QS, Barnett JV, Wasserman DH, Bedimo RJ, Butt AA, Marconi VC, Sico JJ, Tindle HA, Bonaca MP, Aday AW, Freiberg MS. Microvascular disease, peripheral artery disease, and amputation. *Circulation* 140: 449– 458, 2019. doi:10.1161/CIRCULATIONAHA.119.040672.
36. Behroozian A, Beckman JA. Microvascular disease increases amputation in patients with peripheral artery disease. *Arterioscler Thromb Vasc Biol* 40: 534–540, 2020. doi:10.1161/ATVBAHA.119.312859.
37. Anderson CP, Pekas EJ, Park. SY. Microvascular dysfunction in peripheral artery disease: is heat therapy a viable treatment? *Int J Environ Res Public Health* 18: 2384,

2021. doi:10.3390/ijerph18052384.

38. Harris RA, Nishiyama SK, Wray DW, Richardson RS. Ultrasound assessment of flow-mediated dilation. *Hypertension* 55: 1075–1085, 2010. doi:10.1161/HYPERTENSIONAHA.110.150821.
39. Allen JD, Miller EM, Schwark E, Robbins JL, Duscha BD, Annex BH. Plasma nitrite response and arterial reactivity differentiate vascular health and performance. *Nitric Oxide* 20: 231–237, 2009. doi:10.1016/j.niox.2009.01.002.
40. Harris LM, Faggioli GL, Shah R, Koerner N, Lillis L, Dandona P, Izzo JL, Snyder B, Ricotta JJ. Vascular reactivity in patients with peripheral vascular disease. *Am J Cardiol* 76: 207–212, 1995. doi:10.1016/s0002-9149(99)80066-6.
41. Maruhashi T, Nakashima A, Matsumoto T, Oda N, Iwamoto Y, Iwamoto A, Kajikawa M, Kihara Y, Chayama K, Goto C, Noma K, Higashi Y. Relationship between nitroglycerine-induced vasodilation and clinical severity of peripheral artery disease. *Atherosclerosis* 235: 65–70, 2014. doi:10.1016/j.atherosclerosis.2014.04.012.
42. Fronek A, Allison M. Noninvasive evaluation of endothelial activity in healthy and diseased individuals. *Vasc Endovascular Surg* 48: 134–138, 2014. doi:10.1177/1538574413508229.
43. Fronek A, DiTomasso DG, Allison M. Noninvasive assessment of endothelial activity in patients with peripheral arterial disease and cardiovascular risk factors. *Endothelium* 14: 199–205, 2007. doi:10.1080/10623320701547158.
44. Rossi M, Cupisti A, Perrone L, Mariani S, Santoro G. Acute effect of exercise-induced leg ischemia on cutaneous vasoreactivity in patients with stage II peripheral artery disease. *Microvasc Res* 64: 14–20, 2002. doi:10.1006/mvre.2002.2393.
45. Rossi M, Bertuglia S, Varanini M, Giusti A, Santoro G, Carpi A. Generalised wavelet analysis of cutaneous flowmotion during post- occlusive reactive hyperaemia in patients with peripheral arterial obstructive disease. *Biomed Pharmacother* 59: 233–239, 2005. doi:10.1016/j.biopha.2004.01.008.
46. Englund EK, Langham MC, Ratcliffe SJ, Fanning MJ, Wehrli FW, Mohler ER 3rd, Floyd TF. Multiparametric assessment of vascular function in peripheral artery disease: dynamic measurement of skeletal muscle perfusion, blood-oxygen-level

- dependent signal, and venous oxygen saturation. *Circ Cardiovasc Imaging* 8: e002673, 2015. doi:10.1161/CIRCIMAGING.114.002673.
47. Chen HJ, Roy TL, Wright GA. Perfusion measures for symptom severity and differential outcome of revascularization in limb ischemia: preliminary results with arterial spin labeling reactive hyperemia. *J Magn Reson Imaging* 47: 1578–1588, 2018. doi:10.1002/jmri.25910.
 48. Jones S, Chiesa ST, Chaturvedi N, Hughes AD. Recent developments in near-infrared spectroscopy (NIRS) for the assessment of local skeletal muscle microvascular function and capacity to utilise oxygen. *Artery Res* 16: 25–33, 2016. doi:10.1016/j.artres.2016.09.001.
 49. Vardi M, Nini A. Near-infrared spectroscopy for evaluation of peripheral vascular disease. A systematic review of literature. *Eur J Vasc Endovasc Surg* 35: 68–74, 2008. doi:10.1016/j.ejvs.2007.07.015.
 50. Ma KF, Kleiss SF, Schuurmann RCL, Bokkers RPH, Ünlu€ Ç, De Vries JPM. A systematic review of diagnostic techniques to determine tissue perfusion in patients with peripheral arterial disease. *Expert Rev Med Devices* 16: 697–710, 2019. doi:10.1080/17434440.2019.1644166.
 51. Ha DM, Carpenter LC, Koutakis P, Swanson SA, Zhu Z, Hanna M, DeSpiegelaere HK, Pipinos II, Casale GP. Transforming growth factor- β 1 produced by vascular smooth muscle cells predicts fibrosis in the gastrocnemius of patients with peripheral artery disease. *J Transl Med* 14: 39, 2016. doi:10.1186/s12967-016-0790-3.
 52. Pipinos II, Judge AR, Selsby JT, Zhu Z, Swanson SA, Nella AA, Dodd SL. The myopathy of peripheral arterial occlusive disease: part 1. functional and histomorphological changes and evidence for mitochondrial dysfunction. *Vasc Endovascular Surg* 41: 481–489, 2007. doi:10.1177/1538574407311106.
 53. Pipinos II, Judge AR, Selsby JT, Zhu Z, Swanson SA, Nella AA, Dodd SL. The myopathy of peripheral arterial occlusive disease: part 2. oxidative stress, neuropathy, and shift in muscle fiber type. *Vasc Endovascular Surg* 42: 101–112, 2008. doi:10.1177/1538574408315995.
 54. Wang WZ, Anderson G, Fleming JT, Peter FW, Franken RJ, Acland RD, Barker J.

- Lack of nitric oxide contributes to vasospasm during ischemia/reperfusion injury. *Plast Reconstr Surg* 99: 1099–1108, 1997. doi:10.1097/00006534-199704000-00028.
55. Ganesh T, Zakher E, Estrada M, Cheng HM. Assessment of micro-vascular dysfunction in acute limb ischemia-reperfusion injury. *J Magn Reson Imaging* 49: 1174–1185, 2019. doi:10.1002/jmri.26308.
56. Klausner JM, Paterson IS, Valeri CR, Shepro D, Hechtman HB. Limb ischemia-induced increase in permeability is mediated by leukocytes and leukotrienes. *Ann Surg* 208: 755–760, 1988. doi:10.1097/0000658-198812000-00014.
57. Suval WD, Duran WN, Boric MP, Hobson RW 3rd, Berendsen PB, Ritter AB. Microvascular transport and endothelial cell alterations preceding skeletal muscle damage in ischemia and reperfusion injury. *Am J Surg* 154: 211–218, 1987. doi:10.1016/0002-9610(87)90181-4.
58. Farber A, Eberhardt RT. The current state of critical limb ischemia: a systematic review. *JAMA Surg* 151: 1070–1077, 2016. doi:10.1001/jamasurg.2016.2018.
59. Kalogeris T, Baines CP, Krenz M, Korthuis RJ. Ischemia/reperfusion. *Compr Physiol* 7: 113–170, 2016. doi:10.1002/cphy.c160006.
60. Hart CR, Layec G, Trinity JD, Kwon OS, Zhao J, Reese VR, Gifford JR, Richardson RS. Increased skeletal muscle mitochondrial free radical production in peripheral arterial disease despite preserved mitochondrial respiratory capacity. *Exp Physiol* 103: 838–850, 2018. doi:10.1113/EP086905.
61. Makris KI, Nella AA, Zhu Z, Swanson SA, Casale GP, Gutti TL, Judge AR, Pipinos II. Mitochondriopathy of peripheral arterial disease. *Vascular* 15: 336–343, 2007. doi:10.2310/6670.2007.00054.
62. Pipinos II, Sharov VG, Shepard AD, Anagnostopoulos PV, Katsamouris A, Todor A, Filis KA, Sabbah HN. Abnormal mitochondrial respiration in skeletal muscle in patients with peripheral arterial disease. *J Vasc Surg* 38: 827–832, 2003. doi:10.1016/S0741-5214(03)00602-5.
63. Pipinos II, Swanson SA, Zhu Z, Nella AA, Weiss DJ, Gutti TL, McComb RD, Baxter BT, Lynch TG, Casale GP. Chronically ischemic mouse skeletal muscle exhibits myopathy in association with mitochondrial dysfunction and oxidative damage. *Am J*

Physiol Regul Integr Comp Physiol 295: R290–R296, 2008.

doi:10.1152/ajpregu.90374.2008.

64. Thompson JR, Swanson SA, Haynatzki G, Koutakis P, Johanning JM, Reppert PR, Papoutsi E, Miserlis D, Zhu Z, Casale GP, Pipinos II. Protein concentration and mitochondrial content in the gastrocnemius predicts mortality rates in patients with peripheral arterial disease. *Ann Surg* 261: 605–610, 2015. doi:10.1097/SLA.0000000000000643.
65. Pipinos II, Shepard AD, Anagnostopoulos PV, Katsamouris A, Boska MD. Phosphorus 31 nuclear magnetic resonance spectroscopy suggests a mitochondrial defect in claudicating skeletal muscle. *J Vasc Surg* 31: 944–952, 2000. doi:10.1067/mva.2000.106421.
66. Marbini A, Gemignani F, Scoditti U, Rustichelli P, Bragaglia MM, Govoni E. Abnormal muscle mitochondria in ischemic claudication. *Acta Neurol Belg* 86: 304–310, 1986.
67. Bhat HK, Hiatt WR, Hoppel CL, Brass EP. Skeletal muscle mitochondrial DNA injury in patients with unilateral peripheral arterial disease. *Circulation* 99: 807–812, 1999. doi:10.1161/01.cir.99.6.807.
68. Murphy MP. How mitochondria produce reactive oxygen species. *Biochem J* 417: 1–13, 2009. doi:10.1042/BJ20081386.
69. Jansson E, Johansson J, Sylve'n C, Kaijser L. Calf muscle adaptation in intermittent claudication. Side-differences in muscle metabolic characteristics in patients with unilateral arterial disease. *Clin Physiol* 8: 17–29, 1988. doi:10.1111/j.1475-097x.1988.tb00258.x.
70. Larsen S, Nielsen J, Hansen CN, Nielsen LB, Wibrand F, Stride N, Schroder HD, Boushel R, Helge JW, Dela F, Hey-Mogensen M. Biomarkers of mitochondrial content in skeletal muscle of healthy young human subjects. *J Physiol* 590: 3349–3360, 2012. doi:10.1113/jphysiol.2012.230185.
71. Kim K, Anderson EM, Scali ST, Ryan TE. Skeletal muscle mitochondrial dysfunction and oxidative stress in peripheral arterial disease: a unifying mechanism and therapeutic target. *Antioxidants (Basel)* 9: 1304, 2020. doi:10.3390/antiox9121304.
72. Brass EP, Hiatt WR. Acquired skeletal muscle metabolic myopathy in

atherosclerotic peripheral arterial disease. *Vasc Med* 5: 55–59, 2000.

doi:10.1177/1358836X0000500109.

73. Khattri RB, Kim K, Thome T, Salyers ZR, O'Malley KA, Berceci SA, Scali ST, Ryan TE. Unique metabolomic profile of skeletal muscle in chronic limb threatening ischemia. *J Clin Med* 10: 548, 2021. doi:10.3390/jcm10030548.
74. Curtis SE, Vallet B, Winn MJ, Caufield JB, King CE, Chapler CK, Cain SM. Role of the vascular endothelium in O₂ extraction during progressive ischemia in canine skeletal muscle. *J Appl Physiol (1985)* 79: 1351–1360, 1995. doi:10.1152/jappl.1995.79.4.1351.
75. Hoppeler H, Vogt M, Weibel ER, Fluëck M. Response of skeletal muscle mitochondria to hypoxia. *Exp Physiol* 88: 109–119, 2003. doi:10.1113/eph8802513.
76. Baron-Menguy C, Toutain B, Cousin M, Dumont O, Guihot AL, Vessie'res E, Subra JF, Custaud MA, Loufrani L, Henrion D. Involvement of angiotensin II in the remodeling induced by a chronic decrease in blood flow in rat mesenteric resistance arteries. *Hypertens Res* 33: 857–866, 2010. doi:10.1038/hr.2010.83.
77. Muller MD, Drew RC, Blaha CA, Mast JL, Cui J, Reed AB, Sinoway LI. Oxidative stress contributes to the augmented exercise pressor reflex in peripheral arterial disease patients. *J Physiol* 590: 6237– 6246, 2012. doi:10.1113/jphysiol.2012.241281.
78. Ross AJ, Gao Z, Luck JC, Blaha CA, Cauffman AE, Aziz F, Radtka JF 3rd, Proctor DN, Leuenberger UA, Sinoway LI, Muller MD. Coronary exercise hyperemia is impaired in patients with peripheral arterial disease. *Ann Vasc Surg* 38: 260–267, 2017. doi:10.1016/j. avsg.2016.05.135.
79. Comerota AJ, Throm RC, Kelly P, Jaff M. Tissue (muscle) oxygen saturation (StO₂): a new measure of symptomatic lower-extremity arterial disease. *J Vasc Surg* 38: 724–729, 2003. doi:10.1016/s0741-5214(03)01032-2.
80. McDermott MM, Ferrucci L, Gonzalez-Freire M, Kosmac K, Leeuwenburgh C, Peterson CA, Saini S, Sufit R. Skeletal muscle pathology in peripheral artery disease: a brief review. *Arterioscler Thromb Vasc Biol* 40: 2577–2585, 2020. doi:10.1161/ATVBAHA.120.313831.